CORNELL UNIVERSITY
Center for Radiophysics and Space Research
ITHACA, N. Y.

CRSR 462

The Dust Belts of Mars

Steven Soter

Laboratory for Planetary Studies
Cornell University
Ithaca, N.Y. 14850

CORNELL UNIVERSITY

CENTER FOR RADIOPHYSICS AND SPACE RESEARCH

Ithaca, N.Y.

August, 1971

CRSR 462

The Dust Belts of Mars

Steven Soter

Laboratory for Planetary Studies

Cornell University

Ithaca, N.Y. 14850

ABSTRACT

From the unrelated facts that Mars is subjected to a flux of asteroidal projectiles and that it has two very small satellites, an elementary analysis leads to the proposition that the planet possesses an orbiting dust belt system, previously unsuspected. Furthermore, the satellites themselves should have surfaces resembling that of the Moon. Factors bearing on the evolution of an orbiting debris system are discussed, leading to some speculations concerning the origin and structure of the rings of Saturn.

INTRODUCTION

The Martian satellites Phobos and Deimos must be subjected to the same flux of projectiles which produced the craters on Mars itself. Most of the debris from hypervelocity impact is ejected at velocities high enough to escape the weak gravitational fields of the two small moons but not fast enough to escape from orbiting around Mars. In fact very little of the debris is ejected at more than half the satellite orbital velocities. As a result, most of it is initially distributed in orbits clustered toroidally about that of each satellite of origin.

The material in these belts is subject to continuous recapture by and asteroidal ejection from the satellites, to steady "leakage" out of the Mars system, and to size-dependent orbital degradation by the Poynting-Robertson effect. If the balance of these opposing mass transfer rates is ever such that a critical space density of debris builds up, then the toroidal distribution will reach an instability. The critical level is attained when the frequency of interparticle collisions dominates the behavior of the dust, causing it to collapse into a thin ring system.

The apparent absence of such a ring system for Mars allows upper limits to be estimated for both the asteroidal impact flux and the mass of any Martian dust belts. This in turn allows us to evaluate the observability of and space vehicle hazards presented by the orbiting debris.

The ejecta from Martian satellites spend some time in orbit rather than making simple ballistic trajectories as on the moon but the end product should be comparable. The surfaces of Phobos and Deimos should be covered with an equilibrium layer of debris similar to that on the moon.

Application the the general model to the Saturn ring system suggests that this may be a case of toroidal instability. The source of the ring material would be the meteoritic erosion of a satellite situated in the Cassini gap. Reasons why this instability might be attained for Saturn and not for Mars are discussed.

HYPERVELOCITY PROJECTILES IN MARS SPACE

The dominant source of debris impacting Mars is the group of Mars asteroids, i.e., those asteroids having a common range of heliocentric distances with that planet (Öpik, 1966). Since the elimination of an asteroid by Mars is a random statistical process, we can express the present number of Mars asteroids as

$$N(t) = N(0)\ e^{-t/T},$$

where N(0) is the number available t years ago and T is the characteristic survival time. Öpik (1963) used a recent list of 34 Mars asteroids to calculate an average $T = 6 \times 10^9$ years which, being comparable to the age of the solar system suggests that Martian cratering has gone on more or less continuously over geological time to the present.* He also showed that 78.9% of the Mars asteroids are eliminated by actual impact with the Martian surface while most of the remainder are injected into earth space (the Apollo group).

Since the depletion rate is

$$dN/dt = - N/T,$$

the number of asteroids eliminated in time Δt by actual im-

---

*Twenty years ago, E. J. Öpik (1951) in a classic study first developed the expressions for the lifetimes of stray bodies in the solar system against collisions with the planets. On this basis, he predicted that the surface of Mars must be heavily cratered.

pact with Mars is

$$\Delta N = f \frac{N}{T} \Delta t \ , \qquad (1)$$

where f = 0.789. It is assumed that Mars asteroids of all sizes follow the same distribution of orbits and therefore have the same average T (except for the smaller grains which are affected by radiation pressure and drag). Thus (1) remains valid whether ΔN and N refer to the totality of Mars asteroids or to any given size range subset, like the 34 that are large enough to be observed.

In order to determine from the sizes of the visible Mars asteroids the number in any size range, we employ a power law size distribution. Let the total number of objects with radius greater than or equal to R be expressed as

$$N_S(R) = \nu \left(\frac{Z}{R}\right)^S \ , \qquad (2)$$

where ν and Z are constants to be fit and S is the population index. The observed cumulative numbers for the Mars asteroids are plotted logarithmically as the points in Figure 1. Observational selection has evidently depleted the numbers below a radius of a few kilometers. Fitting a straight line (assumed to represent the true distribution) is impossible, but at least a range of curves can be "anchored" in the largest numbers, which are assumed to be complete. There are 5 Mars asteroids of radius $\geq$ 17 km, and the corresponding point in Figure 1 is used for normalization of three selected power laws. Thus we set ν = 5 and Z = 17 km in (2).

The population index S = 1.6 is thought by Öpik (1966) to be the most probable for the Mars asteroids, with S = 2 as an upper limit. This is based on the statistics of observable asteroids in general. Hartmann (1969) has shown that this range is characteristic of singly fragmented basalt blocks. Extensive grinding however always raises the value. It is thus possible that the smaller asteroids have an even larger population index. Dohnanyi (1969) derives a value near S = 2.4 for steady state grinding of asteroidal debris. The number of Mars asteroids and therefore the flux of impact projectiles is extremely sensitive to S. Figure 1 indicates, for example, that the cumulative number with radii greater than 1 cm varies by five orders of magnitude over the range of S values examined.

Substituting N_S into (1), the cumulative number of Mars asteroids of radius $\geq R$ that impact the planet in the time interval Δt is

$$\Delta N_S = f \frac{N_S}{T} \Delta t \ .$$

Turning this around and setting $\Delta N_S = 1$, the average time interval between two impact events of a given size on Mars is

$$\Delta t = \frac{T}{f N_S} \ . \qquad (3)$$

The time interval between equivalent impacts on a smaller body in Mars space, like a satellite, is of course much longer. It increases nearly as the ratio of the surface areas

$$k(r) = (R_\sigma / r)^2 \ , \qquad (4)$$

where $R_{♂}$ and r are the radii of Mars and the smaller target, respectively.

Gravitational focusing of debris and partial shielding of the satellites by Mars might at first be thought to even further decrease the rate of impacts on the satellites with respect to Mars. These effects, however, are negligible. To illustrate focusing, the angular deflection γ of an asteroid in passing a planet is given by (Öpik, 1963)

$$\tan(45^\circ + \frac{\gamma}{4}) = (1 + \frac{2GM}{xU^2})^{1/2} , \qquad (5)$$

where G and M are the gravitational constant and the planet's mass, x is the distance of the asteroid's closest approach to the planet's center, and U is their unperturbed relative velocity in units of the planet's orbital velocity. For asteroids crossing Mars, the average U is 0.429. Substituting this into (5), the maximum deflection for a surface grazing Mars asteroid, with $x = R_{♂}$, is only $\gamma_{max} = 12^\circ$. The difference between the projectile flux at the Mars surface and at the satellite distances can thus be neglected.

As for shielding, the fractional solid angle subtended by Mars as seen from Phobos is only about 3% and it is even less for Deimos. If this is also neglected, the simple ratio of surface areas (4) is sufficient to scale equivalent impact intervals from Mars to a satellite.

The size of Phobos is now known from a picture of it obtained by Mariner 7 (Smith, 1970). Although not spherical, its "radius" is about 10 km. Using this in (4), $k = 1.15 \times 10^5$

for Phobos. The size of Deimos remains unobserved but since it is about 4 times less bright than Phobos, its k should be about 4 times as large, or 6.4×10^5, assuming the same reflectivities.

The time interval between impacts by asteroids of radius equal to or greater than R against a Mars satellite of radius r_o is now found. Multiplying (3) by (4) and substituting N_S from (2), we express it as

$$t = \frac{T}{f\nu} \left(\frac{R\delta}{r_o}\right)^2 \left(\frac{R}{Z}\right)^S \quad . \tag{6}$$

Figure 2 displays t(R) logarithmically for Phobos (solid lines) and Deimos (dashed lines) for three values of S. Note that the time required between Mars satellite impacts by asteroids in the ten to few hundred meter radius range is of the order of the age of the solar system. Actually this is not quite accurate because it assumes that the flux rate of asteroids has remained constant throughout geological time. In fact the population of Mars asteroids has been steadily diminishing with the characteristic survival time T. This means that Z is not constant but was somewhat larger in the past. To get around this, we try a somewhat different approach.

Using the characteristic survival times of the different Mars asteroid orbits, Öpik (1965) has estimated the "original" number of such bodies. He finds that the ratio of the number that have impacted the Martian surface in 4.5×10^9 years to the currently surviving number is $\theta = 1.32$. Using

this, we can write a self-evident expression for the cumulative number of asteroids of radius ≥ R that have struck a Mars satellite of radius r_o in the age of the solar system:

$$N = \theta N_S(R)/k(r_o) \ , \qquad (7)$$

where $N_S(R)$ is the currently extant number. To find the size of the largest asteroid ever to have struck a Mars satellite, set N =1 and substitute the expressions for $N_S(R)$ and $k(r_o)$ into (7) to solve for its radius

$$\hat{R}_S = Z(\theta\nu)^{1/S}\left(\frac{r_o}{R_\sigma}\right)^{2/S} \ , \qquad (8)$$

where we note that $\theta\nu = 6.6$ and recall that Z = 17 km. Some values are listed below.

Table 1: Radius of largest asteroid hitting a satellite

S	$\hat{R}_S$ (in meters) for Phobos	$\hat{R}_S$ (in meters) for Deimos
1.6	38	16
2.0	130	65
2.4	290	160

These values are about 50% larger than those read off Figure 2, as expected, because they account for the larger asteroidal flux in the past.

Now the asteroids corresponding to the largest radii in the above table are only of order 10^{-4} times the mass of Phobos or Deimos. But a hypervelocity projectile would have to possess <u>at least</u> 10^{-4} times the mass of a target rock to com-

pletely shatter it (Wetherill, 1967). There is thus no difficulty for objects like Phobos and Deimos surviving catastrophic destruction by a single impact in 4.5×10^9 years.

In order to assess the effect of steady erosion by the many smaller hypervelocity asteroidal fragments, we calculate the total mass impacting a satellite in the age of the solar system. To obtain the number of asteroids with radii in the range R to R + dR that impact a satellite of radius r_o in 4.5×10^9 years, insert the expression for $N_S(R)$ into (7) and differentiate; thus,

$$dN = - \frac{\theta \nu}{k} S Z^S R^{-S-1} dR \ .$$

The collective mass of all projectiles in this size range is

$$dM = \frac{4}{3} \pi \rho R^3 dN \ ,$$

so the total incident projectile mass is

$$M_S = \frac{4}{3} \pi \rho \frac{\theta \nu}{k} \frac{S}{3-S} Z^S (\hat{R}_S)^{3-S} \ .$$

The integration is from the smallest grains stable in the solar system (the size of which is immaterial to the result so long as $S < 3$) to the largest asteroid to have hit the satellite. The radius of the latter, $\hat{R}_S$, is seen to scale the total incident mass. Some values of M_S are listed in Table 2, assuming $\rho = 2.8$ gm cm^{-3} (density of crustal rock). This evaluation uses Z = 17 km, the $\hat{R}_S$ previously tabulated, and the current values of k for either satellite. Of course with substantial erosion, a satellite's surface area was greater

in the past, so that $k = (R_\delta/r_o)^2$, properly weighted over time, should be smaller, hence the corresponding M_S larger. The results of doing without such a correction will show that, to our accuracy, it is probably unnecessary.

Table 2: Total asteroidal mass hitting a Mars satellite

S	M_S	Phobos M_S (gm)	Deimos M_S (gm)
1.6	$\frac{88.5}{k} Z^{1.6} \hat{R}_{1.6}^{1.4}$	7.3×10^{11}	5.5×10^{10}
2.0	$\frac{155}{k} Z^{2.0} \hat{R}_{2.0}$	5.1×10^{13}	6.3×10^{12}
2.4	$\frac{310}{k} Z^{2.4} \hat{R}_{2.4}^{0.6}$	1.2×10^{15}	2.0×10^{14}

Note that M_S is greater for larger S; i.e., the mass is dominated by the smaller particles for larger S.

Now let Γ be the ratio of ejected to incident mass in a hypervelocity impact. According to Marcus (1969) and others,

$$\Gamma \simeq K V_i^2 ,$$

where K is a constant depending on the nature of the target material and V_i is the impact velocity in km sec^{-1}. It is seen that ejected mass is roughly proportional to impact energy. Relevant suggested values of K range from about 5 for solid basalt to more than 500 for unconsolidated grains. Recent experimental results by Braslau (1970) for hypervelocity impact into dry quartz sand can be interpreted as indicating a K of about 100.

The average relative velocity of an asteroid approaching Mars is roughly 10 km sec^{-1} (Öpik, 1963). Choosing $K \simeq 100$, this gives $\Gamma \simeq 10^4$, so the cumulative mass ejected in 4.5×10^9 years by a Martian satellite with an unconsolidated surface is of order $10^4 M_S$. The largest values considered here are obtained for $S = 2.4$. In this case, the cumulative mass ejected from Phobos would be about 10^{19} gm, and from Deimos about 2×10^{18} gm. These values are about 1.0 and 1.4 times the estimated present masses of the respective satellites. Thus, steady erosion by the smaller hypervelocity projectiles should not have removed more mass from Phobos and Deimos than they currently retain. We conclude that these satellites may well have survived in substantially their present condition in Mars orbit since the origin of the solar system.

INITIAL EJECTION OF SATELLITE DEBRIS

Most of the debris ejected from Phobos and Deimos by hypervelocity impacts will have relatively low velocities. Particles spalled from a satellite with a typical ejection velocity v_{ej} will have their orbits confined within a limiting range of distances from Mars. For a given v_{ej}, the minimum attainable pericenter q_1 is reached by particles ejected in the opposite direction from the satellite's orbital velocity; the maximum attainable apocenter q_2 by particles ejected in the prograde direction. These cases are illustrated in Figures 3a and 3b, as scaled to the Phobos orbit. Debris ejected in directions other than tangential to the satellite orbital velocity will have orbits crossing that of the satellite but with pericenter greater than q_1 and apocenter less than q_2.

It will be useful to find the limiting range of distances (q_1, q_2) confining the orbits of particles with a specified satellite ejection velocity v_{ej}. We consider first the inner pericenter bound q_1. Let v be the initial orbital velocity of a particle ejected opposite the satellite's orbital velocity v_o. Then

$$v = v_o - v_{ej} \quad . \tag{9}$$

From the orbital energy integral,

$$v^2 = GM\left(\frac{2}{a_o} - \frac{1}{a}\right) \quad ,$$

where a is the semimajor axis of the particle's independent orbit, given by

$$2a = a_o + q_1 \ ,$$

with a_o the satellite's semimajor axis. Combining these three equations and using the fact that $v_o^2 = GM/a_o$ yields

$$v_{ej} = \{1 - (\frac{2q_1}{a_o+q_1})^{1/2}\} \, v_o \ . \qquad (10)$$

A similar expression relating the outer apocenter bound q_2 to the ejection velocity is readily found to be

$$v_{ej} = \{(\frac{2q_2}{a_o+q_2})^{1/2} - 1\} \, v_o \ . \qquad (11)$$

To be precise, we should take account of the satellite's escape velocity v_{esc}. Thus, instead of (9), the proper expression should be

$$v = v_o - V \ ,$$

where V is the particle's post-escape velocity with respect to the satellite, obtained by energy conservation from

$$V^2 = v_{ej}^2 - v_{esc}^2 \ .$$

The final expression replacing (10) and (11) turns out to be

$$v_{ej} = [\{\pm(\frac{2q}{a_o+q})^{1/2} - 1\}^2 \, v_o^2 + v_{esc}^2]^{1/2} \ , \qquad (12)$$

where q is a generalized orbital extremum (either q_1 or q_2 according to circumstances). This expression is also more general in that the choice of minus sign allows one to repre-

sent retrograde particle orbits (for initial V opposite to and greater than v_o). However the debris fraction ejected at such high velocities is negligible and will not be considered here. Thus, using the plus sign, we note that (12) reduces to (10) and (11) if escape velocity is neglected.

It turns out that the exact expression (12) is only really needed in the case of ejection velocities less than a few times the escape velocity. For Phobos, Smith (1970) assumes a density of 2.8 gm cm^{-3} to get an escape velocity of about 12 m sec^{-1}. Thus for most of the ejecta from asteroidal impact, the approximate expressions are adequate.

In Figure 4, the orbital bounds q are plotted as a function of v_{ej} for both Phobos (solid lines) and Deimos (dashed lines). The upper and lower branches of either curve represent q_2 and q_1 respectively. Thus, for example, debris ejected from Phobos at v_{ej} = 100 m sec^{-1} is confined to excursions within the region between about 2.3 to 3.3 Mars radii (measured from the center of the planet), while debris ejected at the same velocity from Deimos is allowed to get to limiting distances of about 5.2 to 9.4 Mars radii* The Deimos debris has a wider range, of course, because the Martian gravitational field is less confining at its distance.

The smallest pericenter is represented by collision with Mars, or $q_1 = R_\sigma$. Figure 4 indicates that this becomes pos-

---

*Actually the ranges should all be slightly widened to account for the small orbital eccentricities of Phobos and Deimos.

sible with $v_{ej} > 584$ m sec^{-1} for Phobos and $v_{ej} > 670$ m sec^{-1} for Deimos. The largest apocenter is escape from Mars altogether, or $q_2 = \infty$. From (11), this becomes possible for $v_{ej} > 0.414\ v_o$, which is 558 m sec^{-1} for Phobos and 888 m sec^{-1} for Deimos. Note finally in Figure 4 that for $v_{ej} < v_{esc}$, the particle is confined to the satellite.

To determine the general envelope for debris orbits initiated by a given ejection velocity, we need to know the excursion range out of the satellite orbital plane in addition to the q range within it. In Figure 3c, the particle ejection velocity $\vec{v}_{ej}$ and resultant orbital velocity $\vec{v}$ make angles of ε and i, respectively, with the satellite orbital velocity $\vec{v}_o$ (neglecting a small escape velocity correction). The plane of Figure 3c is taken to be normal to the Mars-satellite radius vector. For given values of v_o and v_{ej}, a maximum inclination i for the resultant orbit is obtained if ε is just slightly larger than 90°, i.e., with $\vec{v}_{ej}$ nearly normal to the satellite orbit plane. If, as will be shown, most of the ejected particles have v_{ej} much lower than v_o, then the resulting inclinations i will be very small compared to 90°. In this case the approximation $|\vec{v}| \simeq |\vec{v}_o|$ is valid. This means, in effect, that to find the maximum excursion out of the satellite orbit plane made by a particle with $v_{ej} << v_o$, one may consider circular orbits.

Therefore consider a near circular orbit of semimajor axis a_o inclined by i to the plane of the satellite orbit (essentially the Martian equatorial plane). A particle in

such an orbit at longitude 90° from its intersection with the satellite will be at maximum elevation above the equator plane, given by $b' = a_o \sin i$. From Figure 3c with $v_{ej} << v_o$, $\sin i \approx v_{ej}/v_o$ so that

$$b' = \frac{v_{ej}}{v_o} a_o \ . \qquad (13)$$

Any particle ejected at a given v_{ej} must now have a pericenter $\geq q_1$, an apocenter $\leq q_2$, and an excursion out of the equatorial plane of $\leq b'$. The envelope of all such orbits will be a toroid, the cross section of which is taken to be an ellipse with semimajor axis $a' = (q_2 - q_1)/2$ and semiminor axis b' as given in (13). Figure 5 shows the cross section of a set of such toroids for Phobos and Deimos corresponding to the four values of v_{ej} labeled in m sec^{-1}. The volume of each toroid, being a figure of revolution for an ellipse centered at $(q_1 + q_2)/2$, is readily found to be

$$V(v_{ej}) = \tfrac{1}{2} \pi^2 (q_2^2 - q_1^2)\, b' \ .$$

The choice of an elliptical cross section, of course, involves an approximation, but one adequate to our present needs.

A key point in the discussion is the fact that the bulk of the debris created in hypervelocity impact has a relatively low average ejection velocity. Gault *et al.* (1963) fired projectiles at about 6.25 km sec^{-1} into solid basalt and plotted the cumulative mass ejected faster than a given velocity.*

---

*Their plot is more accessibly reproduced by Arnold (1965).

They found that less than 1% of the debris had ejection velocities exceeding 1 km sec^{-1}. Although the total ejecta mass scales as the impact energy, the relative mass ejected within a given range of v_{ej} (as long as $v_{ej} \lesssim 1$ km sec^{-1}) is fairly insensitive to the impact velocity.

Some the the data from Gault et al. are indicated along the upper edge of Figure 4. This shows, for example, that less than 1% of the ejecta from Phobos or Deimos has sufficient velocity to hit Mars (or to escape altogether). Most of it remains in orbits close to those of the satellites. Again, from Figure 4, about 70% of the debris mass from a hypervelocity impact into solid basalt has ejection velocities of less than 100 m sec^{-1}. If the Phobos and Deimos surfaces were solid rock, then more than 70% of the impact debris would initially be confined to orbits within the 100 m sec^{-1} toroids shown in cross section in Figure 5.

However, it is unlikely that these satellite surfaces are solid rock. For one thing, a small though significant portion of the debris will have ejection velocities even less than the 12 m sec^{-1} escape velocity of Phobos. In addition, as will be shown, much of the escaped debris will eventually reimpact the satellite at low enough velocities to allow recapture. The satellite surfaces should thus be fragmented, resembling that of the moon.

No data are as yet published, but Gault (personal communication, 1971) indicated that for hypervelocity impact into unconsolidated granular rock,ejection velocities are even

lower than for solid rock targets. Therefore the 150 m sec^{-1} contours in Figure 5 perhaps contain as much as 90% of all debris initially ejected from Phobos and Deimos.

The Mars asteroids have an average unperturbed relative velocity when approaching the planet of about 10 km sec^{-1}, as mentioned before. The Martian gravitational field increases this slightly when an asteroid is within striking distance of a satellite. Finally the orbital velocity of the satellite itself (2.14 km sec^{-1} for Phobos and 1.35 km sec^{-1} for Deimos) will somewhat augment or diminish the final impact velocity to the extent that the collisions are "head-on" or "overtaking", respectively. Thus on the average, a satellite's leading hemisphere will be hit both harder and more often than its trailing hemisphere. A greater mass of ejecta will accordingly have a component of v_{ej} directed forward rather than backwards. Consequently, there will be more debris having orbits initially larger than that of the satellite of origin as opposed to smaller. Finally, from Kepler's Second Law, an orbiting particle spends more time near apocenter than pericenter. The net result of all this is that the outer part of each toroid represented in Figure 5 will contain a substantially greater debris density than the inner part. At least that will be the case for the debris as initially ejected, before radiation drag and collisional interaction take effect.

STABILITY OF DUST BELT CONFIGURATION

The average rate of mass injection from a Martian satellite into the orbiting debris complex may be represented as

$$F_S = \frac{\Gamma M_S}{T_\odot} , \tag{14}$$

where, it is recalled, Γ is the ratio of ejecta to projectile mass and M_S (previously tabulated as a function of the asteroidal population index S) is the total projectile mass incident on a satellite over the age of the solar system. The latter is denoted by $T_\odot = 4.5 \times 10^9$ years. The input rate F_S must be balanced against the various processes that remove debris in order to determine the steady state population and extent of the orbiting debris complex. Removal by satellite recapture is a crucial mechanism and the only one considered here which is independent of particle size. It is essentially a random statistical process. A particle ejected from a satellite at v_{ej} is confined within a toroid of volume V. If the particle does not substantially interact with other debris before next encountering the satellite, its relative velocity on approaching the satellite will be of order v_{ej}. We shall interpret the situation by analogy with a "particle in a box" of volume V; it is bouncing randomly about with velocity v_{ej}; somewhere inside the box is a stationary target of cross section πr_o^2 (the satellite). In this case, the characteristic time between collisions of the particle with the target is

$$\tau_o = \frac{V}{\pi r_o^2 v_{ej}} . \tag{15}$$

Wetherill (1967) has shown that the results of such an approximate calculation are in reasonable agreement with the exact analytical solution in the case of collisions among asteroids.

Below are provided some values of the volume $V/V_{\sigma'}$ (where $V_{\sigma'} = 1.6 \times 10^{26}$ cm^3 is the volume of Mars) and the secondary collision time τ_o as a function of ejection velocity v_{ej} for both satellites.

Table 3: Confining volume and collision time in dust belts

	Phobos		Deimos	
v_{ej} (m sec^{-1})	$V/V_{\sigma'}$	τ_o (yr)	$V/V_{\sigma'}$	τ_o (yr)
25	0.05	32	2.2	5600
50	0.22	72	8.6	11000
100	0.90	150	35	24000
150	2.0	230	83	40000

The ejection velocity v_{ej} for most of the debris is not more than ~ 150 m sec^{-1}, and is usually much less. When a particle later collides with a satellite at these speeds, it will probably not break unless it is larger than a few cm and hits a solid rock surface. If it hits rock, according to Öpik (1969), such a projectile or its fragments will be reflected at about half the collision velocity, and if it hits unconsolidated debris, the projectile may be reflected at up to 20 or 30% of collision velocity. Or the projectile may simply remain in the hole it makes in the debris, as is the

case for many meteoroid fragments striking the earth's surface with comparable terminal velocities (Krinov, 1960). Whether reflected or buried, the projectile may eject tertiary debris, some of which may even escape the satellite. However the relative velocities should be so low that, as will be shown, this material will very shortly be swept up again by the satellite.

If the particle is not captured in its first collision with the satellite, it will acquire a lower relative velocity which confines it to a smaller toroid. The volume of the toroid is proportional to its elliptical cross section $\pi a'b'$. For low velocities, Figure 3 shows that $2a' = q_2 - q_1$ is nearly linear in v_{ej}, and from (13), $b' \propto v_{ej}$. Therefore, to good approximation, $V \propto v_{ej}^2$ and, from (15), $\tau_o \propto v_{ej}$. This means that whenever a particle is reflected off a satellite, the time τ_o until its next collision is shortened on the average in proportion to the diminishing of its relative velocity.

The ejection velocity is at least halved on each "bounce" and the time until the next collision is shortened accordingly. A particle generated by hypervelocity impact, with an initial ejection velocity of even as much as a few hundred meters per second, should in most cases be recaptured from orbit by a satellite after only a few bounces. Let us write the typical capture time as

$$\tau_c = \beta \tau_o \ , \qquad (16)$$

where β ranges from about unity to perhaps 2 or 3.

Consider a toroidal complex of orbiting debris particles which is not sufficiently dense for the particles to interact with each other. This complex contains a satellite with radius $r_o >> r_{max}$, where r_{max} is the radius of the largest debris particle. The dynamical effect of such a satellite revolving in near circular orbit is to diminish the orbital eccentricities and inclinations of the particles with the larger relative velocities and to capture those particles with lower relative velocities. With no new external generation of debris, the toroidal complex would eventually be contracted and accreted by the satellite. The extent to which this would occur in time t is governed by $\exp(-t/\tau_c)$. With a steady input of debris by asteroidal impacts with the satellite, there would result a nearly steady state equilibrium population of orbital debris and satellite surface debris constantly being recycled.

Whether or not the debris complex is rarified enough to avoid interparticle collisions and thus be governed by satellite capture with time scale τ_c depends both on the population index of the asteroidal projectiles and on the mechanics of ejection. If the asteroidal flux is sufficiently large, then the input rate of ejecta F_S is large. And if the equilibrium debris density in the toroid is sufficient to permit interparticle collisions on a time scale less than τ_c, then the debris orbits tend by momentum exchange to become more circular and less inclined. This decreases the toroid volume, in-

creasing the interparticle collision frequency. The toroid becomes unstable and relaxes into a thin disc.

The particles in such a disc can no longer be directly recaptured by the satellite since the orbits are now concentric. Instead, they must remain in orbit until eliminated by other mechanisms, which operate over a time scale large compared to τ_c. But asteroidal impacts will continue to eject debris from the satellite into the initial toroid and this will continue to "feed" the disc population. The mass of the debris in the disc thus becomes much larger than in the toroid, which constitutes a kind of "halo" about the disc.*

The mass of the ring complex continues to grow until a new equilibrium is achieved with the slower elimination mechanisms. These will be considered in a later section. But first let us examine the stability of an orbiting toroidal debris distribution to determine the conditions beyond which it relaxes into a thin disc.

The average injection rate of debris into orbit, F_S as given in (14), is assumed constant and independent of the nature of the resulting debris system. If F_S is sufficiently low, interparticle collisions are avoided because the satellite itself can accumulate the particles before they attain a critical space density. If in this case, F_S were cut off at

---

*The analogy with stellar galactic populations is not intended to go beyond the purely descriptive.

time t = 0, the debris mass remaining in orbit at time t would be

$$m(t) = m(0)\ \exp(-t/\tau_c) \ ,$$

where τ_c is the characteristic recapture time. The elimination rate would therefore be

$$\dot{m} = -\ m/\tau_c \ .$$

If the input flux were restored, the net rate of change of debris mass would then be

$$dm = F_S dt - (m/\tau_c)\ dt \ . \qquad (17)$$

The solution to this rate equation is

$$m = F_S \tau_c \{1 - \exp(-t/\tau_c)\} \ ,$$

which, for $t >> \tau_c$, asymptotically approaches the steady state mass

$$m \rightarrow F_S\ \tau_c \ .$$

Using (14) and (16), the equilibrium toroidal mass of orbiting debris would then become

$$m_S = \frac{\beta \tau_o}{T_\odot}\ \Gamma\ M_S \ , \qquad (18)$$

where, we recall, β is the number of "bounces" and τ_o the average time interval between particle-satellite collisions (as listed in Table 3), $T_\odot$ is the age of the solar system, Γ the ejecta to projectile mass ratio, and M_S the total pro-

jectile mass incident on a satellite in time $T_\odot$, depending on the asteroidal population index S.

It is important to keep in mind that (18) is valid only if the resulting m_S does not exceed the critical mass for toroidal instability. This is determined as follows. We adopt the simplifying assumption that an orbit is randomized if a particle accumulates collisions with λ times its own mass in less time than is required to collide with the satellite. By "randomized" we mean that the particle undergoes sufficient momentum exchange that its orbital inclination and eccentricity are substantially diminished. This is essentially a random walk situation, and since most of the impacts are with many smaller particles, the factor λ is perhaps not more than, say, 2 or 3.

Let a particle of radius r and mass $\tilde{m}$ encounter an accumulated mass $\lambda\tilde{m}$ in traversing a volume δV through the toroid in time τ_λ. The relative velocity between particles will be taken as v_{ej}, the same as with the satellite. If m_S/V is the average space density in the toroid, then the mass encountered in collisions during such a traverse is

$$\lambda\tilde{m} = \frac{m_S}{V}\,\delta V = \frac{m_S}{V}\,\pi r^2 v_{ej}\tau_\lambda \ .$$

Substituting for V from (15),

$$\lambda\tilde{m} = m_S\left(\frac{r}{r_o}\right)^2 \frac{\tau_\lambda}{\tau_o} \ ,$$

where r_o is the radius of the originating satellite. This may be rewritten as

$$\frac{\tau_\lambda}{\tau_o} = \frac{4}{3}\,\pi\rho\lambda\,\frac{r_o^2}{m_S}\,r\ .$$

The condition for instability in the toroid, as previously defined, is $\tau_\lambda < \tau_o$. Let the radius r at which $\tau_\lambda = \tau_o$ be denoted r'. Then the critical particle size for toroidal instability is

$$r' = \frac{3m_S}{4\pi\rho\lambda r_o^2}\ .$$

Substituting for m_S from (18), we have

$$r' = \frac{3\beta\tau_o\,\Gamma\,M_S}{4\pi T_\odot\rho\lambda r_o^2}\ . \qquad (19)$$

Those orbiting particles in the toroid having $r < r'$ will tend to relax into a thin disc configuration. Larger particles will initially remain in the toroidal "halo".

A table of select values for r' is provided for illustrative purposes (the values of the parameters chosen are simply "best guesses"). Using $\beta \sim 2$, $\lambda \sim 2$, $\Gamma \sim 10^4$, $\rho = 2.8$ gm cm^{-3}, and choosing typical values for τ_o (from Table 3) of 100 years for Phobos and 20,000 years for Deimos, we have, respectively, $r_P' \sim 1.9\times10^{-17}M_S$ and $r_D' \sim 1.5\times10^{-14}M_S$. The M_S are derived from Table 2.

Table 4: Particle radius for toroidal instability

S	r_P'	r_D'
1.6	0.1 μ	8 μ
2.0	10 μ	1 mm
2.4	200 μ	3 cm

We now assume (and this will be justified later) that the particle size distribution in the satellite ejecta is similar to that of the lunar surface material. About half the volume of the Apollo 11 lunar soil sample consists of particles smaller than radius 30μ (Duke et al., 1970). If this were used to interpret the preceding table, it would suggest that for S = 2.0, more than half of the mass in the Phobos toroid would be stable while more than half in the Deimos toroid would relax into a thin disc. For S = 1.6, both toroids would be stable and for S = 2.4, both would collapse.

A thin disc around Mars would probably have sufficient optical thickness to be photometrically detectable from the earth. It therefore appears likely that the toroidal configuration remains stable for Mars, and this would imply a relatively low ejecta input rate, hence a relatively low asteroidal impact flux. The values in Table 4 are much too uncertain to draw any firm conclusions, but it may at least be said that the Deimos toroid is more likely to approach instability than that associated with Phobos.

It is possible that at an earlier epoch, the asteroidal flux was much larger, and the space density of the Martian debris complex exceeded the instability level. At such a time Mars would have possessed a ring system resembling that of Saturn, and perhaps a remnant of it (consisting of the larger particles less affected by the Poynting-Robertson drag) survives today. It is also suggested that the Saturn

ring system may itself be the result of meteoritic erosion of small satellites within it at such a rate that a toroidal configuration is unstable. We will return to this suggestions after examining some of the mechanisms that remove particles from a complex of orbiting debris.

MASS LOSS IN A DEBRIS COMPLEX

A small fraction of the ejecta from a satellite will have velocities sufficient to either collide with Mars or escape altogether from orbiting the planet. As previously indicated (cf. Figure 4), this fraction is probably much less than 1% of the total. A particle either has such an initial ejection velocity, in which case it is lost in its first orbit, or it doesn't, in which case it remains to be removed by other means that work over a longer time scale.

Recapture by the satellite does not remove debris from the complex. It only detains the material until recycled by later impacts. Such impacts of course give the material another chance (still less than 1%) to escape from the Mars system or hit the planet. Thus, recycling results in a small steady loss of debris.

Other loss mechanisms, considered in order of increasing time scale are: radiation pressure, Poynting-Robertson drag, and hypervelocity impact of orbiting debris by small asteroidal particles. Additional processes undoubtedly exist, such as exospheric drag and solar wind erosion, but do not appear to be as important in the present context.

Radiation pressure is the fastest means of removing orbiting debris but it is only effective for the fraction of particles in the smallest size range. It produces periodic perturbations in step with the apparent motion of the sun. If the orbital eccentricity becomes too large, the particle

is lost.

Following the analysis of Peale (1966), the orbital eccentricity of a particle of radius r in a combined planetary gravitational and solar radiation field is

$$e = \frac{9}{16} \frac{P_o S_\odot}{\pi b^2 c \rho r} \left[\frac{a}{GM}(1-e_o^2)\right]^{1/2} \alpha \ ,$$

where P_o and M are the planet's orbital period and mass, G is the gravitational constant, e_o is an arbitrary initial value of e, and α is a parameterized particle orbital eccentricity that oscillates with period P_o, but never exceeds α_{max}. Peale has shown that $1 \leq \alpha_{max} \leq 4$. Inserting the upper bound, with $e_o = 0$, we have for a particle orbiting Mars with semi-major axis a, the limiting value

$$e \leq \frac{2.3 \times 10^{-4}}{\rho r} \left(\frac{a}{R_\sigma}\right)^{1/2} \ .$$

For a particle of radius 100μ and density 2.8 gm cm^{-3} injected into an initially circular orbit in the region of the Martian satellites, solar radiation pressure will induce an oscillating eccentricity not exceeding about 0.2.

For particles smaller than about 10μ, this effect begins to become important. Using the lower bound $\alpha_{max} \geq 1$, we find

$$e_{max} \geq \frac{5.9 \times 10^{-4}}{\rho r} \left[\frac{a}{R_\sigma}(1-e_{max}^2)\right]^{1/2} \ .$$

Since to avoid collisions with Mars, an orbiting particle requires that $e_{max} < 1 - R_\sigma/a$, we find the smallest particle that can remain in orbit has a radius

$$r_{min} = \frac{5.9 \times 10^{-4}}{\rho} \frac{(2-R_\sigma/a)^{1/2}}{1-R_\sigma/a} \ .$$

For particles that can cross the orbits of Phobos or Deimos, r_{min} is about 3μ. Anything smaller than this will collide with the planet or escape from the system in less than one Martian year.

The Poynting-Robertson effect, unlike radiation pressure, is not a conservative periodic perturbation, but involves a steady energy dissipation. For a particle of radius r in circular orbit around a planet, the rate of change of the semimajor axis due to the solar Poynting-Robertson effect is (Peale, 1966; Allan, 1967)

$$\dot{a} = -\frac{9}{4}\frac{1.22S_\odot}{b^2c^2\rho r}a \ , \qquad (20)$$

where $S_\odot = 1.36\text{x}10^6$ erg cm^{-2} sec^{-1} is the solar constant, b is the planet's orbital radius in A.U., c is the speed of light, and ρ is the density of the particle. We have chosen here to augment $S_\odot$ by the factor 1.22 to include the pseudo-Poynting-Robertson effect of solar wind protons (Whipple, 1967). Note that the drag rate diminishes as the orbit contracts, unlike the Poynting-Robertson effect for a particle orbiting the sun, in which case the flux and thus the drag increase with time.

The time interval required to reduce the orbital radius from a_2 to a_1, easily found by solving (20), is

$$t = 1.76\text{x}10^7 \rho r \ln\left(\frac{a_2}{a_1}\right) \text{ years} \ .$$

The characteristic time for this effect to diminish the orbital radius by half ($a_2 = 2a_1$) is thus

$$\tau_{PR} = 1.22 \times 10^{7} \rho r \text{ years} , \qquad (21)$$

where r is in cm. The effect is particle size dependent, removing 100μ particles in as little as 3.4×10^{5} years.

Hypervelocity impact by small asteroidal particles will erode the debris complex as well as the satellites which gave rise to it. A direct adaptation of (6) provides the time interval between collisions with an orbiting particle of radius r by asteroidal grains with radius $\geq r/\eta$. We express it as

$$t_S = \frac{T}{f\nu} \left(\frac{R\sigma}{r}\right)^2 \left(\frac{r/\eta}{Z}\right)^S ,$$

and evaluate this for three asteroidal distributions:

$$t_{1.6} = \frac{1.9 \times 10^{16}}{\eta^{1.6} r^{0.4}} \text{ years}$$

$$t_{2.0} = \frac{6.1 \times 10^{13}}{\eta^{2}} \text{ years}$$

$$t_{2.4} = \frac{2.0 \times 10^{11} r^{0.4}}{\eta^{2.4}} \text{ years} .$$

In these expressions, r is in cm. For S = 1.6, the time between such impacts decreases for increasing target size. Note that for S = 2.0, the probability of a particle being hit by an asteroidal projectile more than $1/\eta$ times its own size is independent of that size. And for S = 2.4, the lifetime actually increases with increasing target size because, although the cross section is larger, the size slope is so steep that there are fewer projectiles with radius $\geq r/\eta$.

For $\eta \lesssim 10$, the projectile has more than 10^{-3} the mass of the debris particle, and this may be sufficient to cata-

strophically explode the latter in a 10 km sec^{-1} impact (Wetherill, 1967). The pulverized residue will however initially remain in orbit, although it will now be more vulnerable to the size-dependent Poynting-Robertson drag and to "winnowing" by radiation pressure.

Elimination of satellite debris by this mechanizm is, in any case, slow. Even for the most efficient flux, a 100μ particle must wait on an average at least $t_{2.4} \approx 10^8$ years to be exploded and long before this, it would have been removed by the Poynting-Robertson drag. Neither will the gradual erosion by accumulated impacts of projectiles less than 1/10 the target size be competetive with the Poynting-Robertson effect. The best it can do is break off ultrafine particles which may be rapidly eliminated by radiation pressure.

OBSERVABILITY AND SPACE VEHICLE HAZARD

The equilibrium mass of a toroidal dust belt for Mars has already been found, in (18), and used to examine the problem of instability and relaxation into a disc population. The steady state mass of such a disc or ring would be larger than that of a toroidal belt because, although the input rate is the same (determined by asteroidal flux), the particles in relatively concentric ring orbits would no longer be directly removed by the satellite. Instead they would be removed by the Poynting-Robertson effect with the time scale $\tau_{PR} > \tau_c$.

The minimum steady state mass of a ring is therefore considerably larger than the maximum stable mass of a toroidal belt, by about the ratio $\Phi = \tau_{PR}/\tau_c$, where τ_c is the characteristic lifetime for capture by a satellite. Now τ_{PR}, unlike τ_c, is size-dependent, but inserting an average particle size of, say, 30μ (characteristic of lunar soil) into (21) yields $\langle\tau_{PR}\rangle \sim 3\times10^5$ years. Then using $\beta \sim 2$ and typical values of τ_o (from Table 3) of 100 and 20,000 years, respectively, for Phobos and Deimos, we get $\langle\Phi\rangle_P \sim 2000$ and $\langle\Phi\rangle_D \sim 10$.

If $\hat{m}_S$ is the maximum steady state mass of a toroidal belt, corresponding to the largest asteroidal population for which it remains stable, then the next largest stable configuration that can exist around a planet is a ring of mass $\langle\Phi\rangle\hat{m}_S$. The intermediate mass range is not found in equilibrium, although it might occur if a reduction in meteoritic flux allows a ring to decay.

In assessing the observability and space vehicle hazard presented by a Mars orbiting debris complex, we tentatively assume that the planet does not possess a ring. Even a ring of miminum mass $<\Phi>\hat{m}_S$ would probably have been detected at low inclination. Therefore the upper limit to the debris mass orbiting Mars is assumed to be $\hat{m}_S$, characterizing the largest stable toroidal dust belt. Such a belt probably constitutes the most that an orbiting space vehicle would have to contend with.

Let us assume that the disc population can be represented by an index s of its own (as opposed to S for the impacting asteroids) and a radius r_{max} for its largest member. Then the number of particles of radius $\geq r$ is

$$n_s(r) = (\frac{r_{max}}{r})^s , \tag{22}$$

and the number in the size range r to r + dr is

$$dn = - s r_{max}^s r^{-s-1} dr \quad ,$$

so that the mass in this range is

$$dm_s = - \frac{4}{3}\pi\rho s r_{max}^s r^{2-s} dr \ .$$

Integration from some r_{min} to r_{max} gives the total mass:

$$s < 3, \quad m_s = \frac{4}{3}\pi\rho \frac{s r_{max}^s}{3-s} (r_{max}^{3-s} - r_{min}^{3-s})$$

$$s = 3, \quad m_s = 4\pi\rho r_{max}^3 \ln(\frac{r_{max}}{r_{min}})$$

$$s > 3, \quad m_s = \frac{4}{3}\pi\rho \frac{s r_{max}^s}{s-3} (\frac{1}{r_{min}^{s-3}} - \frac{1}{r_{max}^{s-3}}) \ .$$

We do not know the population index of the dust belt but we will assume it to be comparable to that of the lunar surface. The justification for this is as follows. The debris is produced by hypervelocity impact into unconsolidated rock. The albedo of Phobos, about the lowest in the solar system at 0.065 (Smith, 1970), should rule out anything else. The ejected debris, rather than making simple ballistic trajectories, spends some time in orbit before returning to the surface of the satellite, but the end result should be the same as for the lunar surface.

The population index of lunar surface debris is not yet well known, and undoubtedly varies somewhat from place to place. The data of Gold et al. (1970) for the fine particles would indicate $s \gtrsim 3$. Hartmann (1969) notes $2.1 \lesssim s \lesssim 3.3$ and Shoemaker et al. (1970) suggest $s \approx 2.4$, respectively, for the Surveyor series and Apollo 11 counts of cm range particles. Accordingly, we will use sample values s = 2.1, 2.7, and 3.3. Some results for m_s, assuming $r_{max} >> r_{min}$ and $\rho = 2.8$ gm cm^{-3} are listed.

Table 5: Mass of a debris population

s	m_s
2.1	$27\ r_{max}^3$
2.7	$106\ r_{max}^3$
3.3	$129\ r_{max}^{3.3}/r_{min}^{0.3} \approx 1260\ r_{max}^{3.3}$

In the case s = 3.3, we have chosen $r_{min} \sim 5\mu$, consistent with the limit set by radiation pressure. If these values of debris population mass (as a function of s) are equated to the steady state mass (as determined by asteroidal flux) expressed by (18), we have

$$m_s \equiv m_S = \beta\tau_o \Gamma \frac{M_S}{T_\odot} \quad , \tag{23}$$

where M_S is the total mass of asteroidal projectiles impacting a satellite in $T_\odot = 4.5 \times 10^9$ years.

We want to use the maximum mass $\hat{m}_S$ consistent with the probable absence of a thin ring around Mars. According to the discussion of Table 4, a toroidal belt would be stable for $S \sim 1.6$ for both satellites but would collapse at $S \sim 2.0$ for Deimos. Since a ring is not observed, we will provisionally assume that the population of Mars asteroids is characterized by $S \sim 1.6$. This agrees well with Öpik's (1966) estimate based on statistics of visible asteroids. Corresponding values of $\hat{m}_S$ from Table 2 and (23) are $160\beta\tau_o\Gamma$ for Phobos and $12\beta\tau_o\Gamma$ for Deimos. Inserting these values and the m_s from Table 5 into (23) allows a solution for r_{max} (in cm, with τ_o in years) as given below.

Table 6: Maximum particle radius in a Martian dust belt

s	Phobos belt	Deimos belt
2.1	$(5.9\,\Gamma\beta\tau_o)^{1/3}$	$(0.45\,\Gamma\beta\tau_o)^{1/3}$
2.7	$(1.5\,\Gamma\beta\tau_o)^{1/3}$	$(0.12\,\Gamma\beta\tau_o)^{1/3}$
3.3	$(0.13\,\Gamma\beta\tau_o)^{1/3.3}$	$(0.01\,\Gamma\beta\tau_o)^{1/3.3}$

The r_{max} required to account for a given mass of debris must increase as s decreases (as the proportion of fines decreases). These r_{max} are left in algebraic form for later use, but numerical values are typically on the order of a few meters.

In order to estimate the optical depth of the dust belt, we need its cumulative geometrical cross section. The differential cross section of all particles in the size range r to r + dr is

$$d\sigma = \pi r^2 dn = - \pi s r^s r_{max}^{1-s} dr \ ,$$

which for s > 2 integrates to

$$\sigma = \frac{\pi s}{s-2} \frac{r_{max}^s}{r_{min}^{s-2}} \ .$$

Again using $r_{min} \sim 5\mu$ and applying the r_{max} from Table 6, the total cross section σ (in cm^2) of the most massive stable dust belt as a function of its population index can be given.

Table 7: Maximum cumulative cross section of a dust belt

s	Phobos belt	Deimos belt
2.1	$3700\ (\Gamma\beta\tau_o)^{0.7}$	$81\ (\Gamma\beta\tau_o)^{0.7}$
2.4	$16000\ (\Gamma\beta\tau_o)^{0.9}$	$340\ (\Gamma\beta\tau_o)^{0.9}$
3.3	$21000\ \Gamma\beta\tau_o$	$1600\ \Gamma\beta\tau_o$

The dust belt should appear brightest when least inclined to the line of sight (i.e., when the Martian equator plane

passes across the earth). If we invoke the simplifying assumption that the space density of debris is constant within a given toroid, then the line of sight with maximum optical depth traverses a distance

$$\ell = 2(q_2^2 - q_1^2)^{1/2} \qquad (24)$$

through the toroid, as shown for the Phobos debris in Figure 6.

Within the bounds of geometrical optics, the optical depth τ_ℓ along such a path is essentially the fraction of the area of observation subtended by any reflecting surface, which may be written as

$$\tau_\ell = (\frac{\sigma}{V})\ell \ .$$

The quantities needed to evaluate this expression are found in Tables 3 and 7, using (24) and Figure 4. For the maximum brightness we insert the σ values corresponding to s = 3.3 (most heavily weighted toward smaller particles of the distributions considered). The resulting values of τ_ℓ are of order 10^{-6} for both satellites. Since the optical depth of the inner edge of the faint C ring of Saturn is of order 10^{-2} (Cook, et al., 1971), we conclude that a Martian dust belt would not be detectable from earth. It might, however, be observable from the planet's surface or from a Mars orbiting vehicle as an equatorial enhancement to the background zodiacal light.

To assess the hazard to an orbiting space vehicle from

the maximum stable Martian dust belt permitted, a provisional list is included of the maximum number of orbiting particles of radius ≥ 1 mm and the number ≥ 1 cm, as determined from (22) with r_{max} values again taken from Table 6.

Table 8: Maximum number of particles ≥ 1 mm in Martian belts

s	Phobos belt	Deimos belt
2.1	$440\ (\Gamma\beta\tau_o)^{0.7}$	$72\ (\Gamma\beta\tau_o)^{0.7}$
2.7	$700\ (\Gamma\beta\tau_o)^{0.9}$	$70\ (\Gamma\beta\tau_o)^{0.9}$
3.3	$260\ \Gamma\ \beta\tau_o$	$20\ \Gamma\ \beta\tau_o$

Table 9: Maximum number of particles ≥ 1 cm in Martian belts

s	Phobos belt	Deimos belt
2.1	$3.5\ (\Gamma\beta\tau_o)^{0.7}$	$.57\ (\Gamma\beta\tau_o)^{0.7}$
2.7	$1.4\ (\Gamma\beta\tau_o)^{0.9}$	$.14\ (\Gamma\beta\tau_o)^{0.9}$
3.3	$.13\ \Gamma\ \beta\tau_o$	$.01\ \Gamma\ \beta\tau_o$

These particles are assumed to be confined within a toroid having an area projected on the equatorial plane of

$$A = \pi(q_2^2 - q_1^2) ,$$

so the areal density (projected on that plane) of particles

with radius ≥ r is

$$w = \frac{n_s(r)}{A} .$$

For the worst case (with regard to a space vehicle) considered here, using s = 3.3 and assuming $\Gamma\beta \sim 2\times10^{4}$ in the 100 m sec^{-1} toroid, some values of w (in cm^{-2}) are listed.

Table 10: Maximum equatorial areal density of Martian belts

	Phobos	Deimos
w(r≥1mm)	4×10^{-10}	4×10^{-10}
w(r≥1cm)	2×10^{-13}	2×10^{-12}

Thus the probability of a 10 m^2 space vehicle impacting a particle larger than 1 mm in a single normal penetration of the Martian equator plane in either satellite dust belt is less than about 4×10^{-5}. With two orbits per day through these belts, a space vehicle should be able to survive for several years before hitting anything larger than sand grains.

If, however, $\Gamma\beta$ is larger by an order of magnitude, the spacecraft lifetime is reduced accordingly. It must also be emphacized that this analysis of dust belt density is based on poorly known parameters and may be in error by orders of magnitude. This section should be regarded more as expository rather than quantitatively reliable.

MASS TRANSFER AND SATELLITE SURFACES

Debris orbiting in a Martian dust belt would appear to be governed by three major processes: (a) continuous recycling of the overwhelming bulk of the material through impact ejection and satellite recapture; (b) steady "leakage" away from the system by the highest energy fraction and by the finer particles subject to radiation pressure; and (c) mass transfer by the Poynting-Robertson effect.

The last named process may have some unusual consequences. We envision the following possible scenario. Debris ejected from Deimos by hypervelocity asteroidal impact initially contributes to the dust belt associated with that satellite. Most particles are likely to be recaptured by Deimos before being removed from its vicinity by the Poynting-Robertson effect. But once recaptured, a particle is given another chance to be ejected by fresh asteroidal impacts, hence another chance to be removed by the Poynting-Robertson effect. The ejection-recapture cycle simply tosses the debris back and forth. Eventually it will leak out of the Mars system altogether or, staying within it, spiral in out of the vicinity of the satellite.

Once the Poynting-Robertson drag has circularized a particle's orbit and reduced the semimajor axis sufficiently to prevent further recapture by Deimos, the particle must continue to spiral inward to the vicinity of Phobos. By the time it approaches Phobos, its orbital eccentricity will

have been sufficiently reduced by drag that the low relative velocity with the satellite assures capture.

Similarly, debris ejected from Phobos by asteroidal impact is mostly recycled through the Phobos dust belt and recaptured, but some is drained away by the Poynting-Robertson effect which in this case will cause it to spiral in to be lost in the Martian exosphere. However, the confining gravitational field closer to Mars reduces the size of the Phobos dust belt (cf. Figure 5) and this makes recapture more likely than in the case of Deimos (cf. Table 3). the result may be that Phobos does not loose much mass to Mars but rather constitutes a "bottleneck" for the debris spiralling in from Deimos. The fact that Phobos appears to be about eight times as massive as Deimos is consistent with this possibility.

Because most of the debris constituting the surface of a Martian satellite should be recycled material that has spent some time in orbit, it is probably deficient in the smaller sizes that are preferentially removed from orbit. Thus its size frequency distribution is expected to depart from a power law with constant population index s for particles smaller than about 5μ due to selective elimination by radiation pressure.

It should be possible to determine observationally whether or not the Martian satellites possess the proposed lunarlike surface debris layer. Such a surface would exhibit an opposition effect and a negative polarization branch. According to Veverka (personal communication, 1971), the

opposition effect should be photometrically detectable from the earth in the case of Deimos. Since Phobos is so close to Mars, however, any opposition effect it displays may be indistinguishable from that due to the bright image of the planet. On the other hand, this would present no difficulty for the case of a detector in an orbiting space vehicle.

SPECULATIONS CONCERNING SATURN'S RINGS

Meteoritic erosion of a small satellite or satellites orbiting within the Saturn ring system may in fact be the source of the ring material. The Saturn ring would then be a degenerate toroidal distribution which has exceeded the instability mass limit, as previously discussed. That such may be the case for Saturn but not for Mars may be due to several factors.

A sufficiently rapid generation of satellite-ejected debris together with a gradual enough removal of it would allow the instability to develop. The flux of cometary or meteoritic particles may, for all we know, be much larger in the region of Saturn than in the inner solar system. Also, Cook and Franklin (1970) estimate that cometary meteoroids bombard Saturn's rings with relative impact velocities averaging about 34 km sec^{-1}. This high speed is due partly to the rapid orbital revolution of the ring particles. It is about three times as fast as the relative impact velocity of Mars asteroids with Phobos and Deimos. Furthermore, hypervelocity impact into ice (the most likely constituent of a Saturn ring satellite) would probably give a larger ejecta to projectile mass ratio than obtains for rock.

But the major difference is that a hypothetical Saturn ring satellite, unlike Phobos or Deimos, lies within the Roche limit of its primary. This subject has been widely misunderstood. The Roche limit is the distance from a planet at

which a body with no internal cohesion would be disrupted by tidal forces. A solid body, if smaller than a certain critical size, would not be broken up inside the Roche limit because its material strength is more important than self-gravity in holding it together. Jeffreys (1947a) discussed this problem and found that an ice satellite with radius less than 100 km would not be broken up at the distance of Saturn's rings.

However, no satellite within the Roche limit can retain an unconsolidated surface. Therefore a hypothetical ring satellite would not be able to sweep up any debris ejected from it. Erosion would simply continue to increase the space density of orbiting material. The only process removing it would be the Poynting-Robertson effect which, however, is smaller for Saturn than for Mars in proportion to the ratio of heliocentric distances squared, a factor of ~40.

According to this model, the Saturn ring system would be in equilibrium between input from satellite ejecta and outflow mainly by Poynting-Robertson drag. There would be no mediation by temporary satellite recapture, the process regulating the dust belts of Mars. A particle ejected from a satellite would soon become entrained in the dense ring, its orbit would be circularized, and even if it again encountered the satellite, it could not be recaptured.

A Saturn ring satellite could also neatly explain the Cassini gap. A number of attempts have been made to account for the radial structure of the rings in terms of resonances

with longitudinal asymmetries in the rotating planet (Allan, 1967) or with the mean motion of the known satellites (most recently by Franklin and Colombo, 1970). The latter especially may well explain some of the ring features but these models are not entirely satisfactory. A small satellite, on the other hand, with an orbital eccentricity of ~0.012, would be quite sufficient to maintain the Cassini gap clear of ring particles.

It would work as follows. Hypervelocity bombardment of a satellite in the gap ejects debris which is soon entrained either in the outer (A) or inner (B) rings of Saturn. The damping effect of interparticle collisions alone tends toward an equilibrium state in which the ring is extremely thin and it does this by spreading radially inwards and outwards in its own plane (Jeffreys, 1947b). Thus particles would be continually edging in to the Cassini gap.

If a particle in nearly circular orbit enters the gap from the inner edge, it will soon be overtaken by the ring satellite near the latter's pericenter. The particle will receive an impulse in the forward direction imparting to it a larger orbital velocity than the satellite has at that distance. This immediately makes the particle's orbit more eccentric than the satellite's, but the pericenters are the same, so the particle's apocenter will lie just past the outer edge of the Cassini gap. Thus half an orbit period after being hit by the satellite near the inner edge of the gap, the particle will find itself entrained at the other side in the A ring where its orbit is soon circularized.

Similarly, a particle entering the gap from outside will soon overtake the satellite at the latter's apocenter and bounce off, leaving it with a smaller orbital velocity than the satellite at that distance, again imparting a larger eccentricity which in half an orbit takes the particle across the gap to the edge of the B ring. The advance of the satellite's line of apsides due to Saturn's oblateness assures that these orbital impulses will occur at all longitudes.

The ability of the satellite to shuttle ring particles back and forth across the Cassini gap depends on the Roche instability in a curious way. For without its effect, the satellite would gradually sweep up the orbiting particles and grow by accretion. The Roche limit prevents this and preserves a clean ice surface off of which the particles easily rebound. It also continues to prevent new satellites from accreting out of the ring--its traditional function.

The relative velocity of a particle in circular orbit colliding with the ring satellite at either edge of the Cassini gap is $\sim$200 m sec^{-1}. This is equivalent to about 5 cal gm^{-1}, which will not melt any ring particles but may break the larger ones. Most of the energy goes into the rebound of the particle or its fragments. These collisions may even somewhat enhance the erosion of the satellite itself.

Over a long period of time, momentum transfer from the many small collisions at apocenter and pericenter will reduce the satellite's eccentricity and work to "close the gap". In addition, since the gap is thought to lie outside the corotating

distance with the body of Saturn, tidal torque will slowly increase the satellite's semimajor axis, resulting in the whole Cassini gap receding from Staurn.

Underlying the exchange of particles across the Cassini gap is a steady one-way net transfer of mass from the outer to the inner ring due to the Poynting-Robertson effect. The smaller particles have the fastest orbital evolution but eventually even the moderate-sized ones spiral into Saturn. Inside the dominant central B ring is the faint C ring, decreasing in brightness toward the planet. The diminution in brightness from the C ring on inward may be due to exospheric and increasingly effective semi-corotating atmospheric drag (this possibility to be further examined at a later date).

The position of the Cassini gap in the Saturn ring system is consistent with the satellite erosion hypothesis. The ejection velocity required to get a particle from a satellite in the gap to the outer edge of the A ring is $\sim$600 m sec^{-1}. This is, within a factor of 2 or 3, the highest ejection velocity to be experienced by any substantial portion of debris from a hypervelocity impact.

Guerin (1970) has produced a remarkable photograph showing a very faint "D ring" separated by a gap from the C ring and extending inward to the planet itself. This inner ring gap may also be produced by a satellite in slightly eccentric orbit, although its limiting size would have to be less than that of a satellite in the Cassini gap to avoid tidal disruption.

The many smaller gaps or bands in the radial structure

of Saturn's rings (cf. Dollfus, 1961) may be explained, on the basis of the present hypothesis, by the presence of additional orbiting ring satellites with smaller size and/or more circular orbits. The orbits of these satellites, including the one in the Cassini gap, may be determined or influenced by resonances with the known satellites. The present hypothesis would then supplement those previously proposed to account for the radial structure of the rings of Saturn.

None of these ring satellites, however, could be directly observed from earth because of their limiting size. To avoid tidal disruption, satellites in the ring may be no larger than about 100 km in radius. This is comparable to the estimated lower bound on the radius of Janus (Dollfus, 1970). And Janus is so faint that it could only be discovered when the rings were presented edgewise to reduce the glare.

Further study and comparison of Saturn's rings and the proposed dust belts of Mars may contribute to our understanding of processes involved in the evolution of the solar system as a whole.

Acknowledgement:

This research was supported by NASA Contract NASA-JPL 952487.

REFERENCES

Allan, R.R. (1967). Resonance effects due to the longitude dependence of the gravitational field of a rotating primary. Planet. Space Sci. 15, 53-76.

Arnold, J.R. (1965). The origin of meteorites as small bodies. III. General considerations. Astrophys. J. 141, 1548-1556.

Braslau, D. (1970). Partitioning of energy in hypervelocity impact against loose sand targets. J. Geophys. Res. 75, 3987-3999.

Cook, A.F., and Franklin, F.A. (1970). The effects of meteoroidal bombardment on Saturn's rings. Astron. J. 75, 195-205.

Cook, A.F., Franklin, F.A., and Palluconi, F.D. (1971). Saturn's rings--a survey. JPL Tech. Memo. 33-488.

Dohnanyi, J.S. (1969). Collisional models of asteroids and their debris. J. Geophys. Res. 74, 2531-2554.

Dollfus, A. (1961). Visual and photographic studies of planets at the Pic du Midi. In "Planets and Satellites" (G.P. Kuiper and B.M. Middlehurst, eds.), pp. 534-571. University of Chicago Press.

Dollfus, A. (1970). Diamètres des planètes et satellites. In "Surfaces and Interiors of Planets and Satellites" (A. Dollfus, ed.), pp. 46-139. Academic Press, London.

Franklin, F.A., and Colombo, G. (1970). A dynamical model for the radial structure of Saturn's rings. Icarus 12, 338-347.

Gault, D.E., Shoemaker, E.M., and Moore, H.J. (1963). Spray ejected from the lunar surface by meteoroid impact. NASA TND-1767.

Gold, T., Campbell, M., and O'Leary, B.T. (1970). Optical and high-frequency electrical properties of the lunar sample. In "Proceedings of the Apollo 11 Lunar Science Conference" (A.A. Levinson, ed.), Vol. 3, pp. 2149-2154. Pergamon Press, New York.

Guerin, P. (1970). The new ring of Saturn. Sky and Tel. 40, 88.

Hartmann, W.K. (1969). Terrestrial, lunar, and interplanetary rock fragmentation. Icarus 10, 201-213.

Jeffreys, H. (1947a). The relation of cohesion to Roche's limit. Mon. Not. Roy. Astron. Soc. 107, 260-262.

Jeffreys, H. (1947b). The effects of collisions on Saturn's rings. Mon. Not. Roy. Astron. Soc. 107, 263-267.

Krinov, E.L. (1960). "Principles of Meteoritics." Pergamon Press, New York.

Marcus, A.H. (1969). Speculations on mass loss by meteoroid impact and formation of the planets. Icarus 11, 76-87.

Öpik, E.J. (1951). Collision probabilities with the planets and the distribution of interplanetary matter. Proc. Roy. Irish Acad. 54 A, 165-199.

Öpik, E.J. (1963). The stray bodies in the solar system. Part 1. Survival of cometary nuclei and the asteroids. Adv. Astron. Astrophys. 2, 219-262.

Öpik, E.J. (1965). Mariner IV and craters on Mars. Irish Astron. J. 7, 92-104.

Öpik, E.J. (1966). The Martian surface. Science 153, 255-265.

Öpik, E.J. (1969). The Moon's surface. Ann. Rev. Astron. Astrophys. 7, 473-526.

Peale, S.J. (1966). Dust belt of the earth. J. Geophys. Res. 71, 911-933.

Shoemaker, E.M., Hait, M.H., Swann, G.A., Schleicher, D.L., Schaber, G.G, Sutton, R.L., Dahlem, D.H., Goddard, E.N., and Waters, A.C. (1970). Origin of the lunar regolith at Tranquility Base. In "Proceedings of the Apollo 11 Lunar Science Conference" (A.A. Levinson, ed.), Vol. 3, pp. 2399-2412.

Whipple, F.L.(1967). On maintaining the meteoritic complex. In "The Zodiacal Light and the Interplanetary Medium" (J.L. Weinberg, ed.), pp. 409-426. NASA SP-150.

FIGURE CAPTIONS

Fig. 1. Cumulative number of Mars asteroids with radius $\geq R$, extrapolated from counts of the larger members for three suggested values of population index S. Inset shows the depletion by observational selection for visible members.

Fig. 2. Average time interval between impacts by a Mars asteroid of radius $\geq R$ into Phobos (solid lines) and Deimos (dashed lines) for the three values of S.

Fig. 3. a) A particle ejected with relatively low velocity v_{ej} opposite a satellite's orbital velocity v_o attains a prograde orbit with pericenter q_1.

b) For ejection in the same direction, orbit is larger than that of the satellite and has apocenter q_2. Scale in (a) and (b) is for orbit of Phobos (radius a_o).

c) In the plane normal to the Mars-satellite radius vector, a particle ejected at angle ε with equatorial plane attains an orbit of inclination i.

Fig. 4. Range of possible pericenter and apocenter distances (in Mars radii) for particles ejected at v_{ej} from Phobos (solid curves) and Deimos (dashed curves). Ejecta fraction data at top is from experimental impacts into solid basalt.

Fig. 5. Cross section of toroidal envelopes containing initial orbits of all debris ejected at velocity $\leq$ values labeled in m sec^{-1} for Deimos dust belt (at right). Same labels apply to smaller Phobos toroids centered at 2.76 $R_{\sigma^{\prime}}$.

Fig. 6. Maximum optical path length ℓ through a dust belt in the equatorial plane.

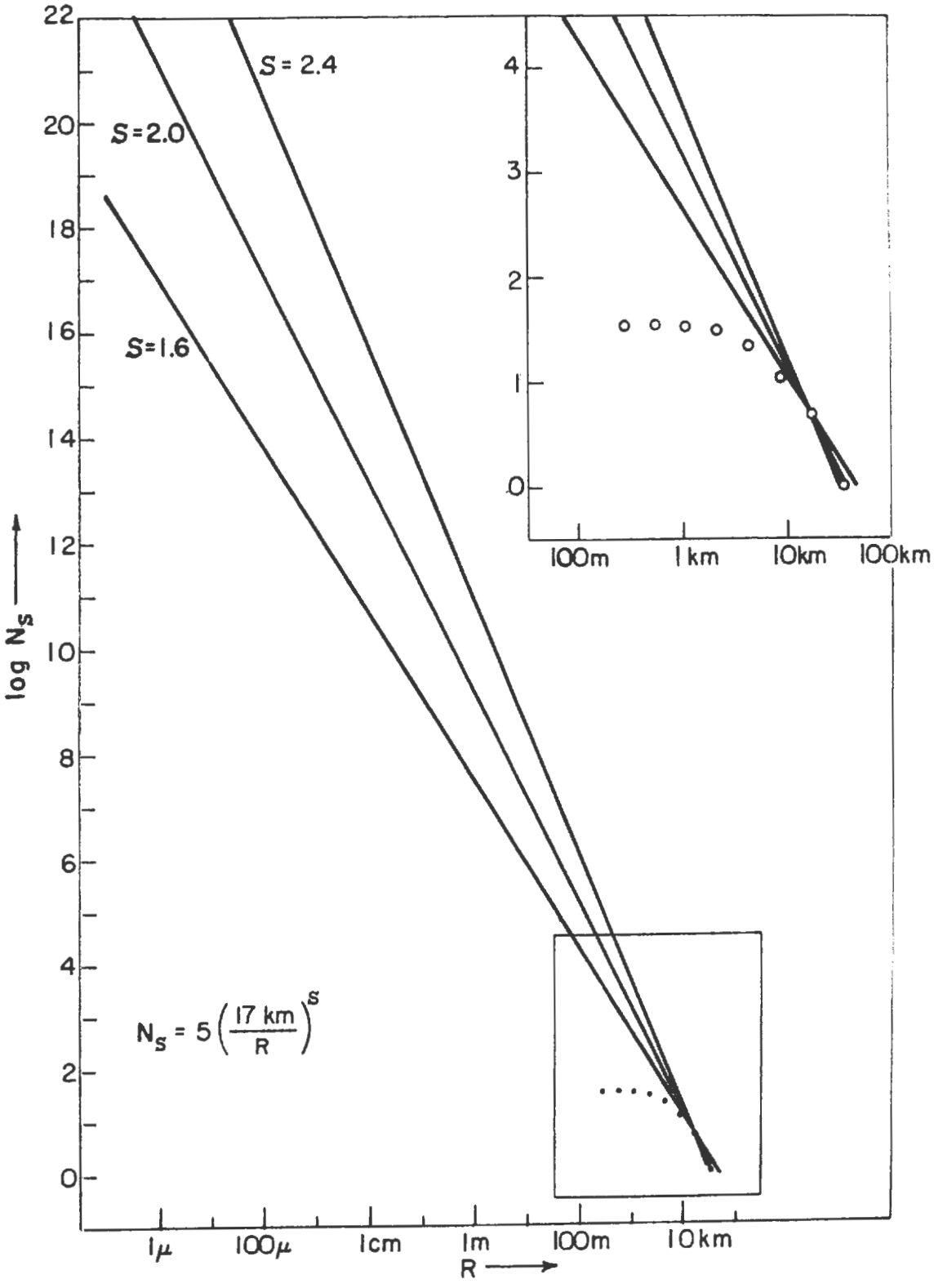
S = 2.4
S=2.0
S=1.6
$N_S = 5\left(\frac{17\ km}{R}\right)^S$
log N_S
R
1μ
100μ
1cm
1m
100m
10km
100m
1 km
10km
100km

Figure 1

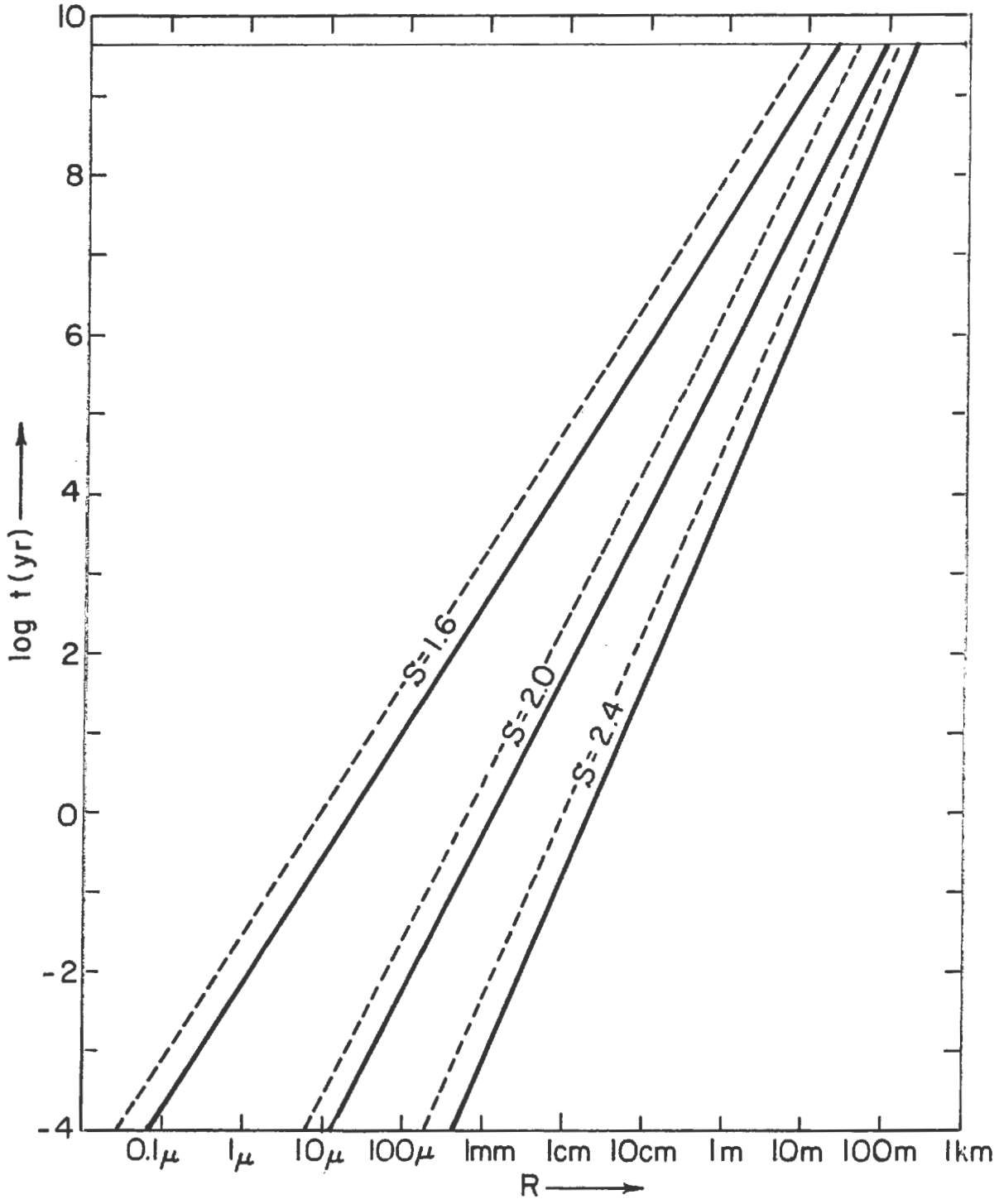
10
8
6
4
2
0
-2
-4
log t (yr)
S=1.6
S=2.0
S=2.4
0.1μ
1μ
10μ
100μ
1mm
1cm
10cm
1m
10m
100m
1km
R

Figure 2

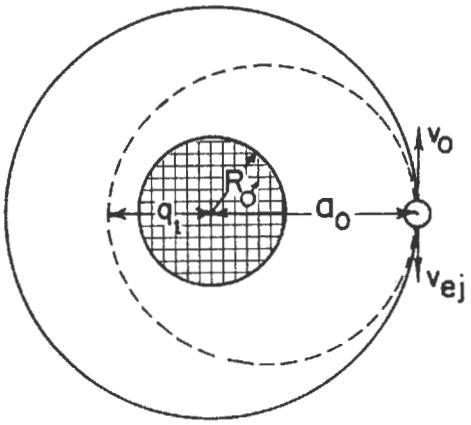

(a)

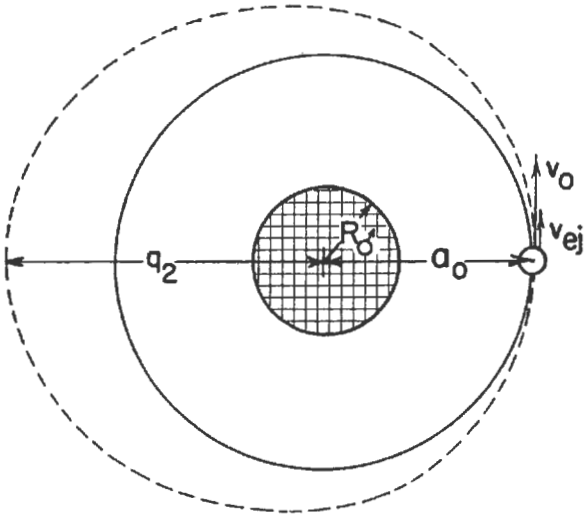

(b)

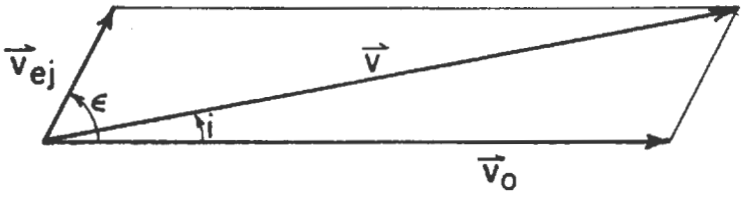

(c)

Figure 3

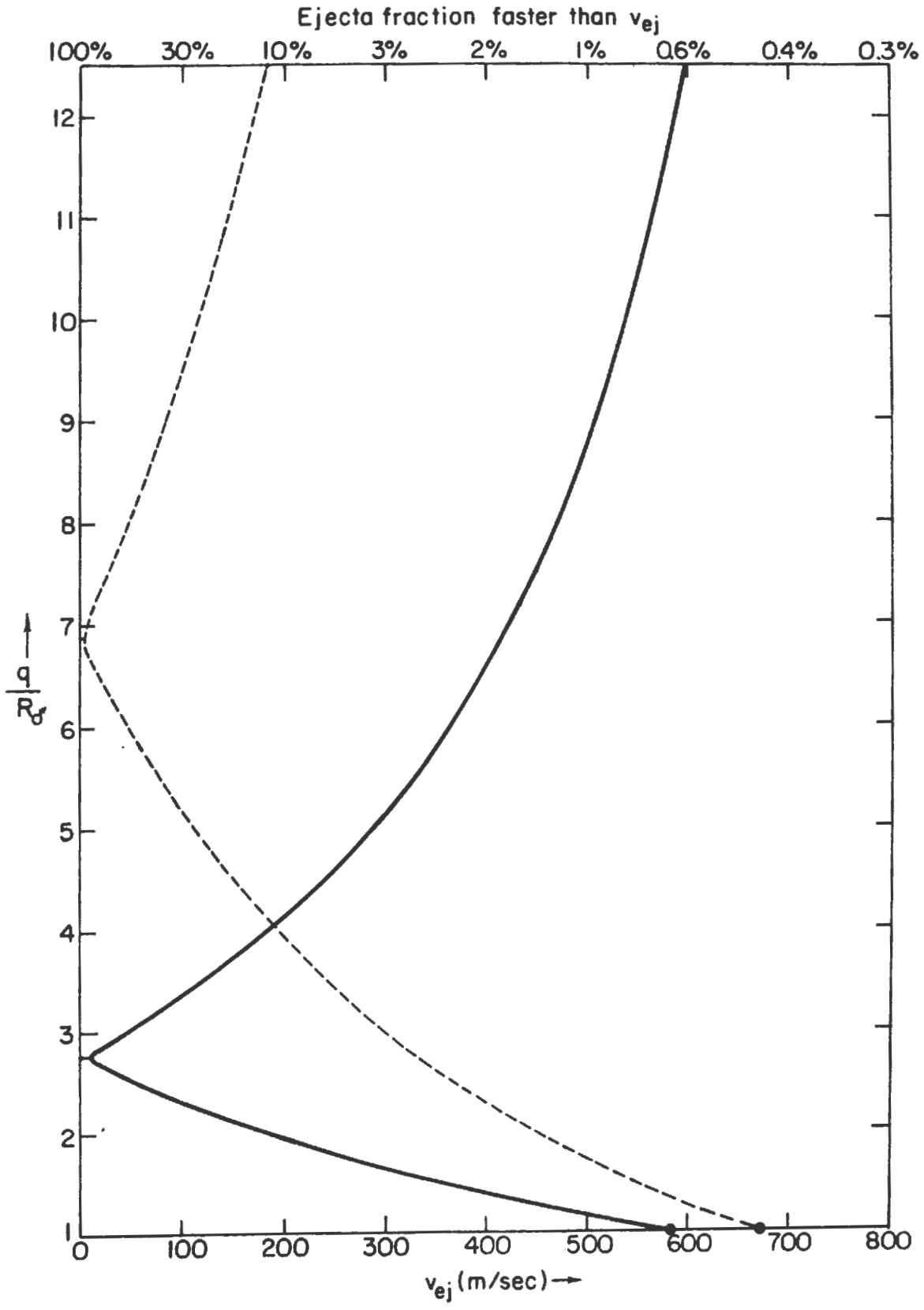
Ejecta fraction faster than v_{ej}
100%
30%
10%
3%
2%
1%
0.6%
0.4%
0.3%
12
11
10
9
8
7
6
5
4
3
2
1
$\frac{q}{R_d}$
0
100
200
300
400
500
600
700
800
v_{ej} (m/sec)

Figure 4

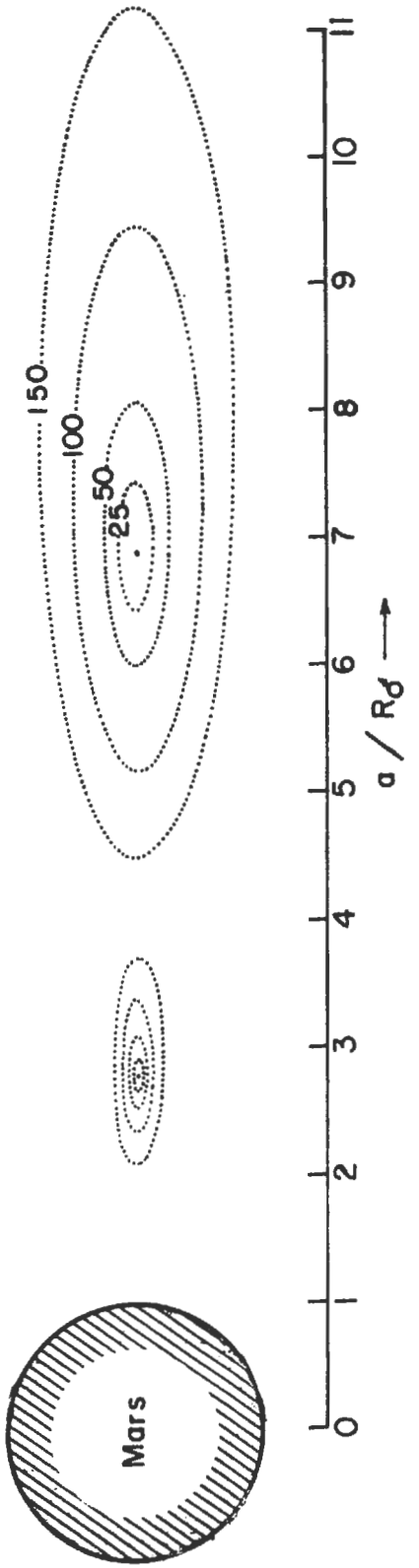

Figure 5

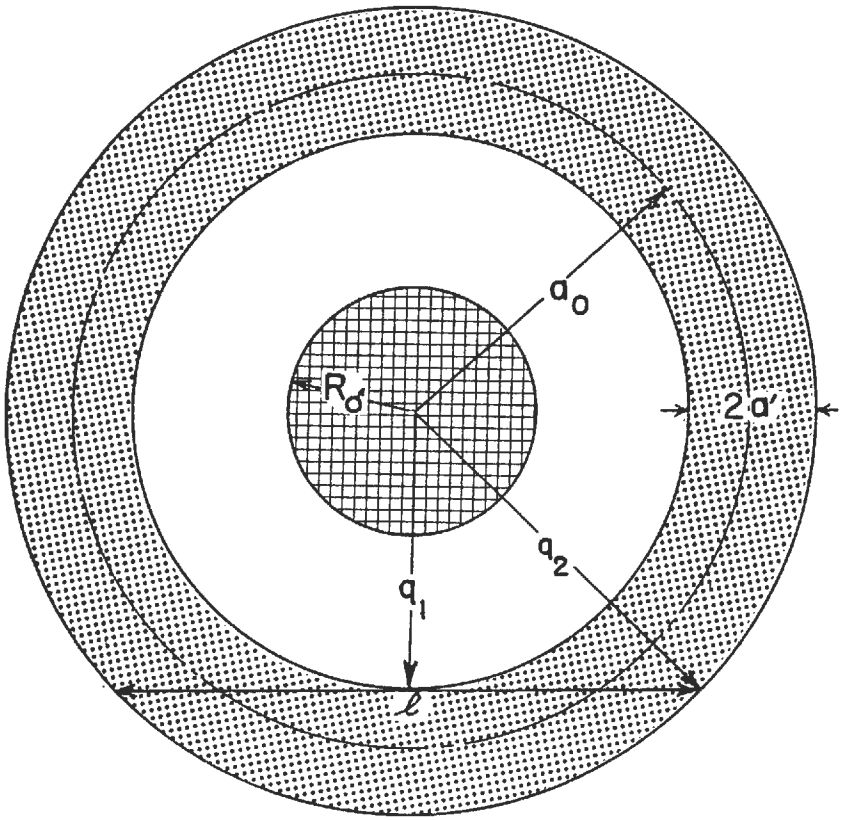

Figure 6